Progress In Electromagnetics Research C, Vol. 122, 141–151, 2022

A Planar Suspended Multiband Yagi Antenna for WLAN, LTE, and 5G Wireless Applications

Sarala S. Shirabadagi and Veeresh G. Kasabegoudar*

Abstract—A planar suspended multiband Yagi antenna suitable for WLAN, LTE, and 5G wireless applications has been presented. The antenna presented here has been optimized to offer operating bands ($S_{11} < -10$ dB) centered at 2.05 GHz, 2.75 GHz, 3.8 GHz, and 6.5 GHz. The proposed antenna has good front to back (F/B) ratios of 14 dB, 13 dB, 12 dB, and 19 dB corresponding to four resonant frequencies. Similarly, the corresponding gain values are 2 dB, 1.3 dB, 3.1 dB, and 3.3 dB. A prototype antenna was fabricated and tested. Except the first resonance which is a single frequency, the other three operating bands offer impedance bandwidths of 3.98% (2.71 GHz–2.82 GHz), 5.48% (3.73 GHz–3.94 GHz), and 19.27% (5.93 GHz–7.195 GHz). Measured results agree fairly with the simulated characteristics of the proposed antenna.

1. INTRODUCTION

Yagi antenna is the most preferred choice for wide range of wireless applications due to its high gain and directional properties [1–4]. However, conventional Yagi antennas pose size constraints for mobile applications. In 1991, Huang and Densmore [5] proposed a planar microstrip-Yagi antenna popularly known as a quasi-Yagi antenna suitable for mobile applications. It unites the advantages of conventional Yagi antenna with microstrip antenna such as light weight, low profile, and ease of fabrication. However, it is well known that the planar microstrip-Yagi antennas offer narrow bandwidth with a poor gain. Therefore, several researchers have addressed these issues and reported numerous innovative techniques to improve performance parameters of quasi Yagi antennas. These include gain improvement [6], bandwidth enhancement [6–14], size reduction, and design of compact antennas [4, 6–8]. A few researchers have reported works on applications specific geometries like WLAN [15, 16], 5G Cellular [17], RF-ID [18], beam steering/wide-beam/dual-beam characteristics [1, 9, 17], etc. More details on various quasi Yagi antennas with respect to feeding methods, driven element type (monopole/dipole), number of dipoles used, and shape of driven element (patch, bow-tie etc.) with their applications can be found in [19].

On the other hand, dual, triple, and multi-band characteristics [8, 20, 21] are more desirable due to the integration of several applications into a single wireless device. In order to fulfill these requirements, several researchers have reported their investigations on antennas with dual, triple, and multi-band characteristics [22–29]. In order to excite multiple resonances/modes, the most popular techniques include the use of multiple driven elements and adding stubs on the driven elements. A compact dual-band antenna with multimodes was proposed in [8]. It uses two driven elements to excite two operating bands with impedance bandwidth of 44% and 115%, respectively. Chen et al. [22] have used split ring resonators to demonstrate the dual-band Yagi antenna. Here, the second resonance is excited by using an additional ring. The presented antenna covers GSM 1800 and ISM 2450 bands with gain of 5.8 dBi and 6.0 dBi, respectively. In another work by [23], a dielectric resonator based quasi Yagi antenna is proposed. It uses a magnetic dipole with differential feed to excite dual modes. Elahi et al. [25] have

Received 23 June 2022, Accepted 26 July 2022, Scheduled 9 August 2022
* Corresponding author: Veeresh G. Kasabegoudar (veereshgk2002@rediffmail.com).
The authors are with the ECE Department, School of Engineering, Central University of Karnataka, Kalaburagi, India.

used two narrowly spaced active/driven elements and truncated-ground for dual-band operation with optimum gain. It operates from 1.71 GHz to 1.9 GHz and 2.5 GHz to 2.7 GHz with gain of 6 and 7 dBi, respectively.

Furthermore, [27] and [28] cover triple band operations, and [29] covers four operating bands. The geometry reported in [28] makes use of two dipoles and stub loading to excite triple bands. The work presented in [29] adopts substrate integrated waveguide (SIW) approach with silicon as the substrate to demonstrate four bands operation. From these works it may be noticed that many of them suffer from the features like offering only two bands or poor front to back ratio (FBR), and complicated design approach.

In this work, a simple conventional Yagi antenna suspended above the ground plane has been designed that offers four resonant bands. It makes use of dual dipoles/driven elements with stub loaded to excite four resonant modes. The proposed antenna has been designed on an easily available low cost FR-4 substrate with the permittivity of 4.4 and height of 1.6 mm. It offers four resonance bands with center frequencies at 2.05 GHz, 2.75 GHz, 3.765 GHz, and 6.705 GHz which are suitable for WLAN, LTE, RF energy harvesting, and 5G wireless services.

Section 2 covers the basic geometry structure of the proposed printed Yagi antenna. Optimization of the proposed design is covered in Section 3. Experimental validation of the fabricated antenna is discussed in Section 4. The work presented here is concluded in Section 5.

2. PROPOSED QUASI YAGI ANTENNA

The geometry structure of the proposed Yagi antenna is shown in Figure 1. The geometry is derived from [11] with necessary changes so as to obtain multiband operation. These changes include the introduction of an air gap, use of an additional substrate on the ground plane, and introduction of stubs

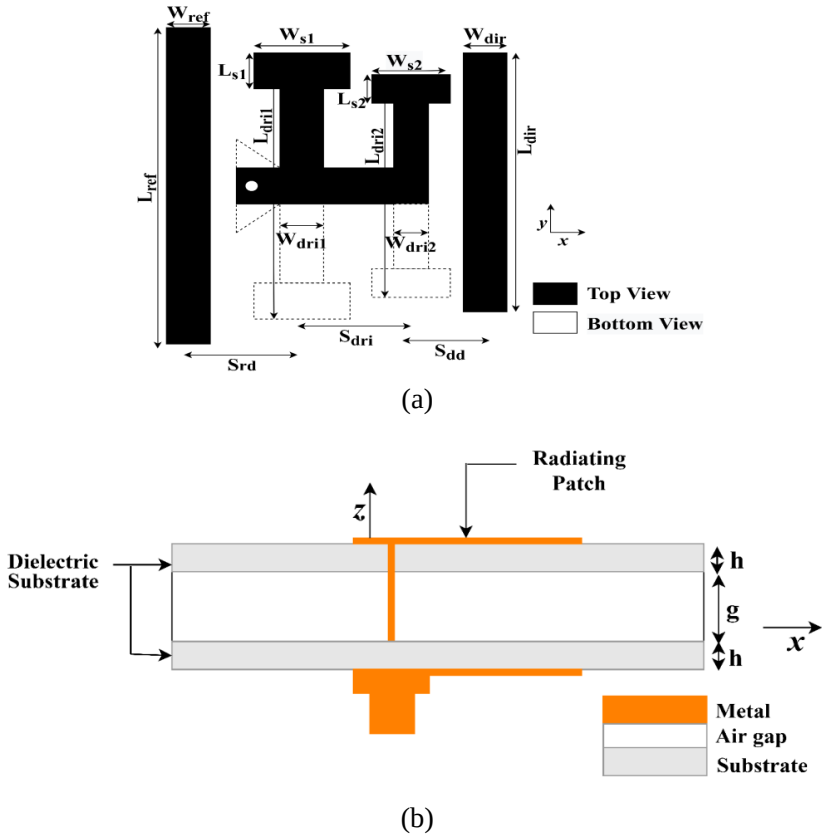

Figure 1. Geometry of the proposed quasi Yagi antenna. (a) Proposed antenna geometry. (b) Cross section view.

on the driven elements. Stubs are added to excite multiple resonances/bands [28]. Two FR-4 substrates are separated by an air gap of 4.5 mm. Upper part of the Yagi antenna is printed on the top substrate (Figure 1(a)), and a lower part is fabricated on the back of the bottom substrate (Figure 1(b)) which also acts as a defective ground structure. A tapered balance to unbalance (BALUN) [11] impedance matching structure is printed along with the lower portion of the proposed design. The tapered line (microstrip to strip-line transition) ensures the transforming unbalanced input to a balanced output [11]. The spacing between the driven elements (S_{dri}), reflector and the first driven element (S_{rd}), and second driven element and the director (S_{dd}) are placed as per the standards of Yagi antenna design, and scaling factors are kept as suggested in [11].

The scaling factor chosen for the design of driven elements is $0.82(= L_n/L_{n-1})$, where L_n is the length of smaller driven element, and L_{n-1} is the length of longer driven element. Further, the spacing factor (σ) was chosen from Equations (1) and (2) [30, 31],

$$0.03 \leq \sigma \leq \sigma_{opt} \tag{1}$$

In (1), the σ_{opt} value is calculated from (2) as,

$$\sigma_{opt} = 0.243\tau - 0.051 = 0.14826\lambda \tag{2}$$

In this work, the spacing factor was varied between 0.12λ and 0.14λ. For the spacing values less than 0.12λ, the stubs of the dipoles touch each other, and for values greater than 0.14λ, the number of resonances will be dropped to two. Hence, an optimum value of 0.133λ was chosen for the proposed antenna design.

3. DESIGN OPTIMIZATION

This section covers the optimization of the antenna geometry proposed in Section 2. It was observed that not all the parameters affect the performance of the proposed antenna. The key parameters which affect the performance of the antenna geometry are the width of air gap (g), spacing between the driven elements (S_{dri}), and the length of stubs (L_{s1}). All these parametric variations are investigated in the subsequent paragraphs. Optimized values are listed in Table 1.

3.1. Airgap Optimization

The air gap shown in Figure 1 was varied from 3.0 mm to 6.0 mm in steps of 0.5 mm. Effects of changing the air gap values are shown in Figure 2. It may be noticed that there are four resonant frequencies at 2.05 GHz, 2.675 GHz, 3.75 GHz, and 6.6 GHz. The optimum value was obtained for an air-gap value of 4.5 mm.

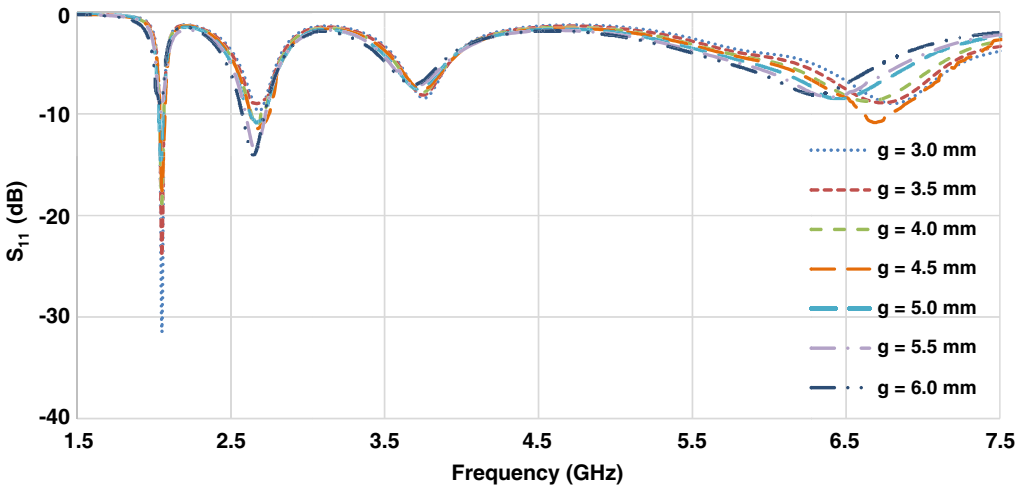

Figure 2. Effect of air gap parameter on return loss characteristics.

3.2. Spacing between the Driven Elements (S_{dri})

In this study, the spacing between the two driven elements was varied from 13.685 mm to 15.685 mm in steps of 0.5 mm. The return-loss characteristics of the same are shown in Figure 3. From the results presented it may be noted that the spacing value of 14.685 mm offers the optimum values.

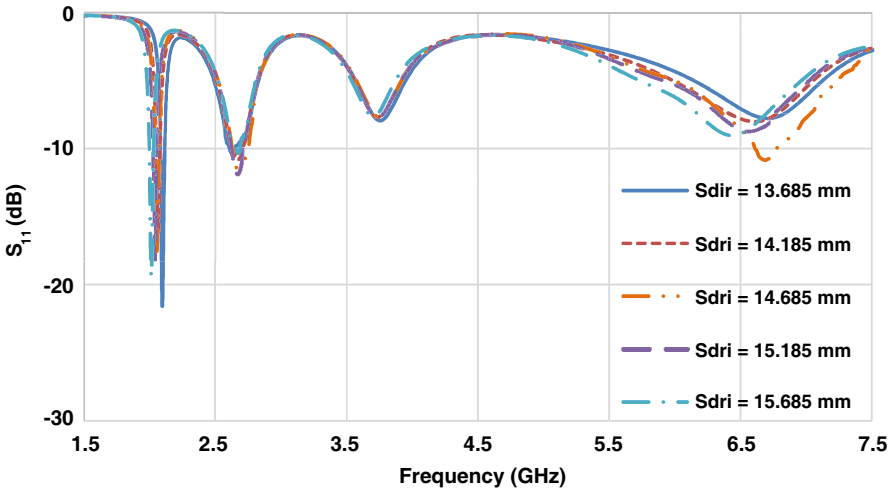

Figure 3. Effect of spacing between the driven elements on return loss characteristics.

Table 1. Dimensions of proposed quasi Yagi antenna (all values are in mm).

Parameter	Values (mm)
Width of driven element 1 (W_{dri1})	5.0
Width of driven element 2 ($W_{dri2} = W_{dri1} * \tau$) ($\tau = 0.82$)	4.1
Length of driven element 1 (L_{dri1})	28
Length of driven element 2 ($L_{dri2} = L_{dri1} * \tau$)	22.96
Length of Stub 1 (L_{s1})	5.0
Length of Stub 2 (L_{s2})	4.1
Total length of driven element 1 ($L_{dri1} + L_{s1} * 2$)	38
Total length of driven element 2 ($L_{dri2} + L_{s2} * 2 = L_{dri1} * \tau$)	31.16
Spacing between driven elements (S_{dri})	14.68
Width of stub 1 (W_{s1})	12
Width of stub 2 (W_{s2})	11.1
Length of reflector (L_{ref})	58
Width of reflector (W_{ref})	5.0
Spacing between reflector and driven element (S_{rd})	12.0
Director Length (L_{dir})	29.45
Width of director (W_{dir})	5.0
Spacing between director and driven element (S_{dd})	8.72
Air gap (g)	4.5

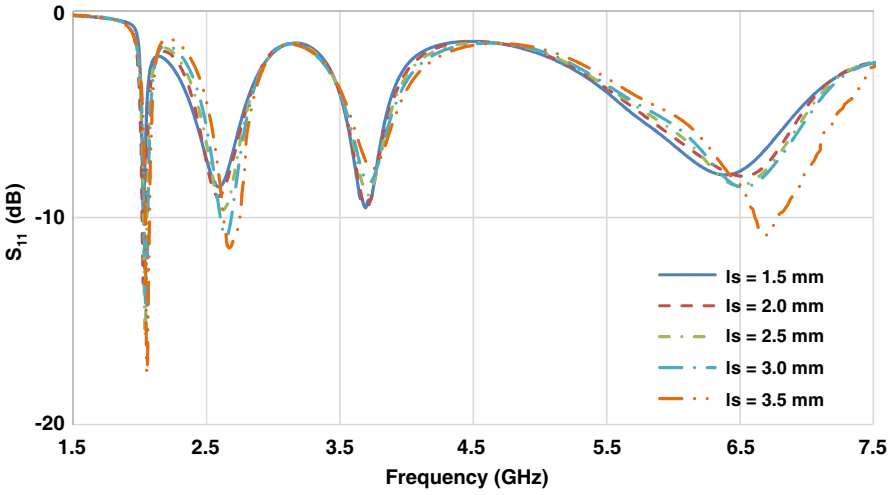

Figure 4. Effect of stub length on return loss characteristics.

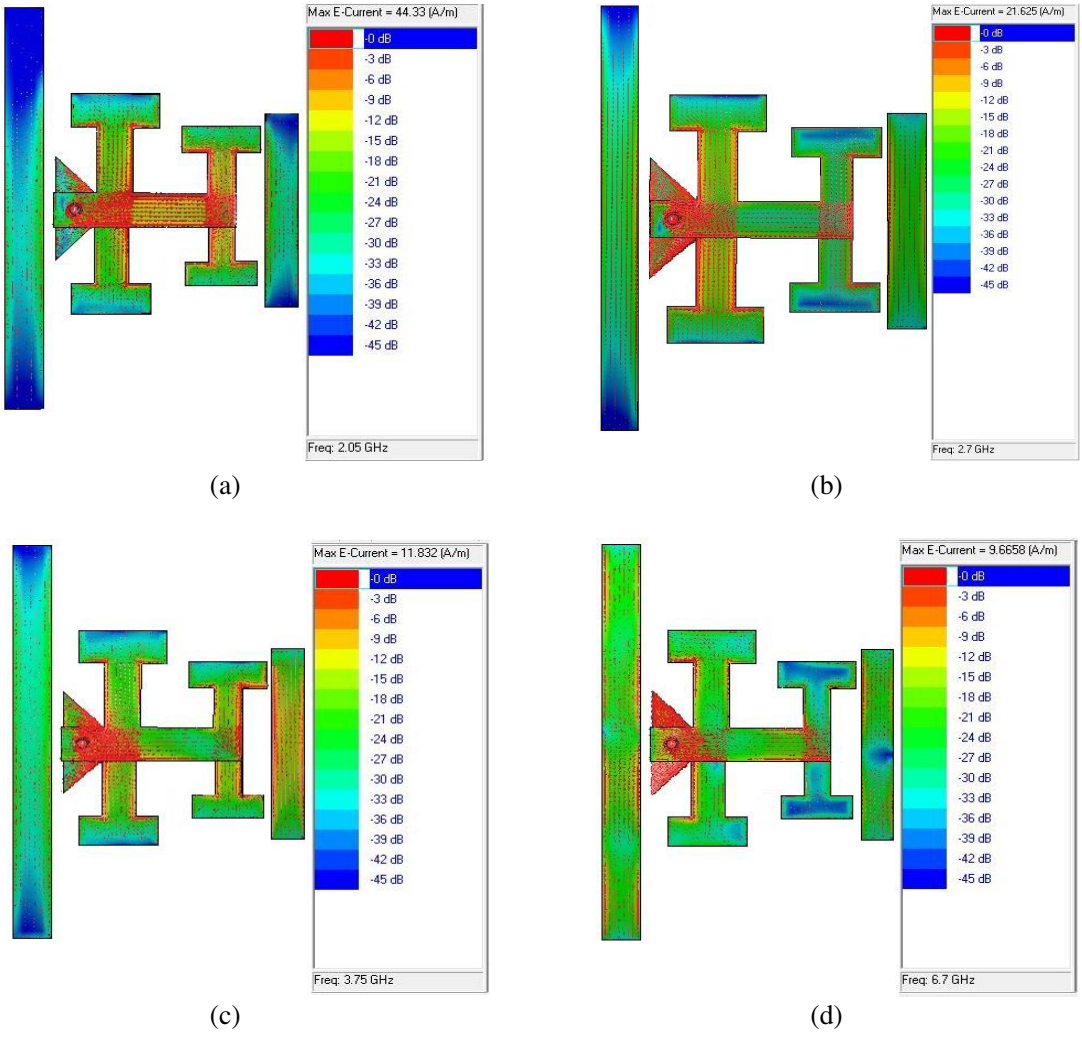

Figure 5. Current distributions at various resonant frequencies. (a) 2.05 GHz, (b) 2.7 GHz, (c) 3.75 GHz, (d) 6.7 GHz.

3.3. Length of Stub (S)

As explained earlier, stubs are added on the driven elements to excite multiple resonances. Stub 1 and stub 2 are placed on top of driven elements 1 and 2, respectively. The scaling factor of 0.82 is used for designing the stub lengths and widths. The dimensional values of these stubs are listed in Table 1. Return loss characteristics of this study are presented in Figure 4. From this study a stub length of 2.5 mm offers an optimum value.

In order to understand the radiation mechanism and modes of the proposed antenna, the current distributions at four resonant frequencies for the optimized geometry are presented in Figure 5. From the current distributions it may be noted that the first resonance frequency is mainly due to the longer driven element, and for this frequency shorter driven element acts as the director (pl. ref. Figure 5(a)). On the other hand, the second resonance is due to smaller driven element, and the longer one acts as the reflector. Further, it may be noticed that the current distributions for remaining resonances shown in Figures 5(c) and (d) are due to harmonics and stubs.

4. EXPERIMENTAL VALIDATION

The optimized design presented in Figure 1 was fabricated on an FR-4 substrate with a relative dielectric constant value of 4.4 and substrate height of 1.56 mm. Antenna return loss parameters were measured using ENA E5063 Keysight network analyzer. Photographs of the specimen antenna geometry and its measurement setup are shown in Figure 6. The comparison of measured and simulated results of S_{11} parameters of the fabricated antenna is shown in Figure 7. From Figure 7 it may be noted that the results agree fairly with simulated data. The measured data exhibit four resonances at 2.05 GHz, 2.69 GHz, 3.87 GHz, and 6.75 GHz. The respective bandwidths of 1^{st}, 2^{nd}, 3^{rd}, and 4^{th} resonance bands are 0.5%, 4%, 5.5%, and 19.5%, respectively. Further, measured gains for these resonant frequencies

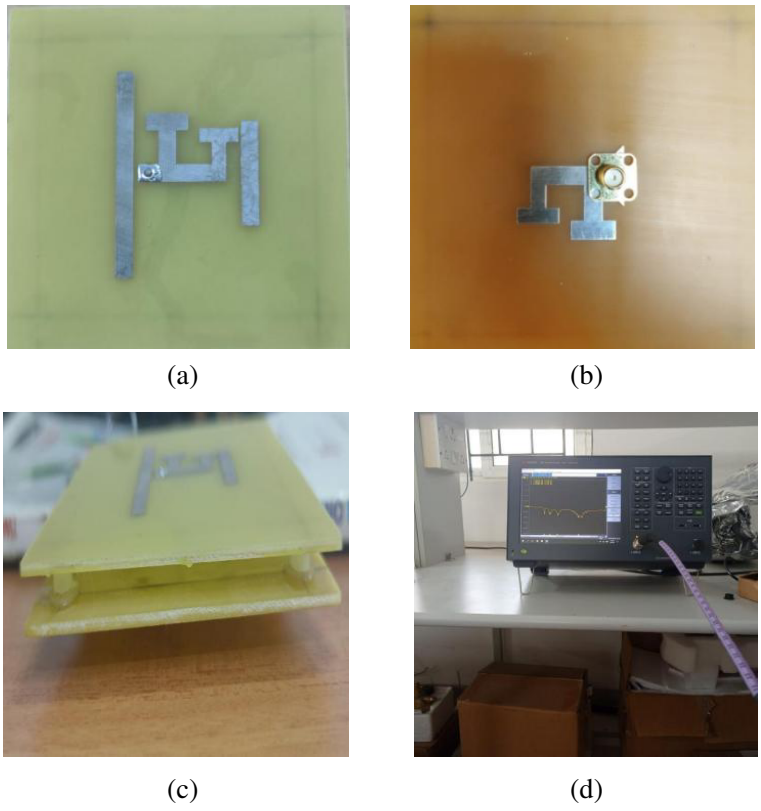

(a) (b) (c) (d)

Figure 6. Fabricated prototype and experimental setup. (a) Top view. (b) Bottom view. (c) Assembled prototype. (d) Screenshot of the measured S_{11}.

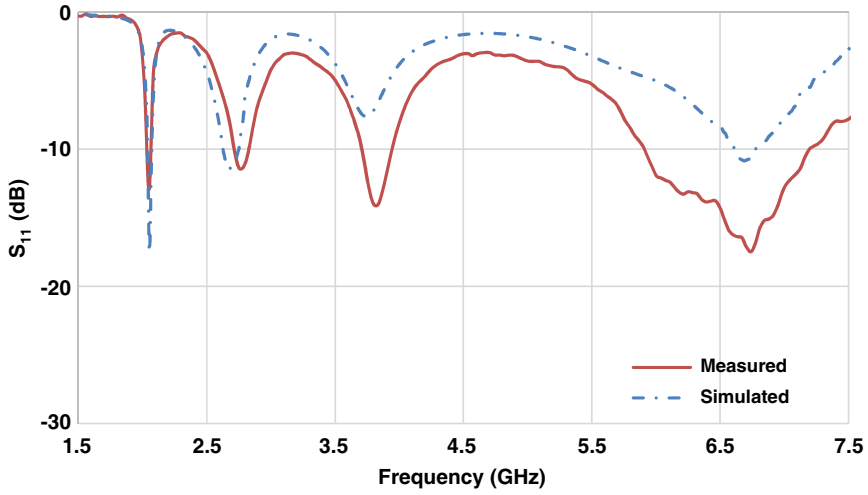

Figure 7. Comparison of simulated and measured return loss characteristics.

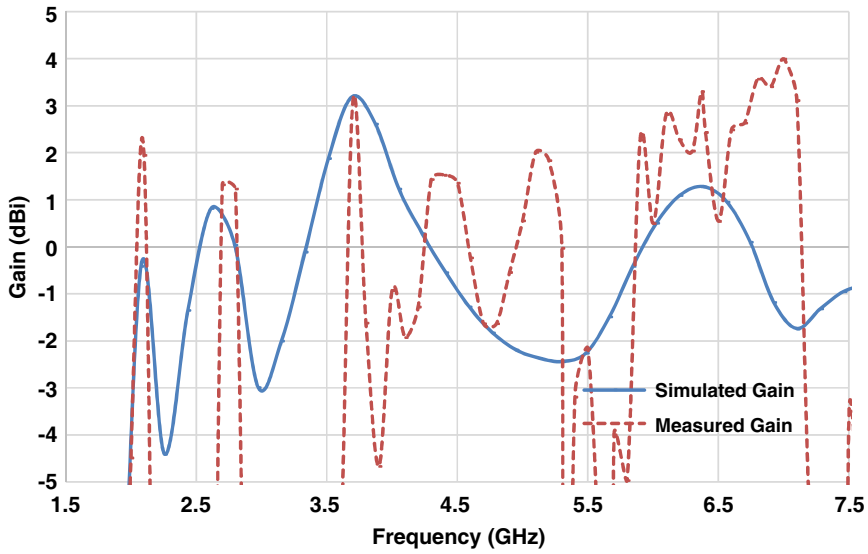

Figure 8. Comparison of simulated and measured gain vs. frequency characteristics.

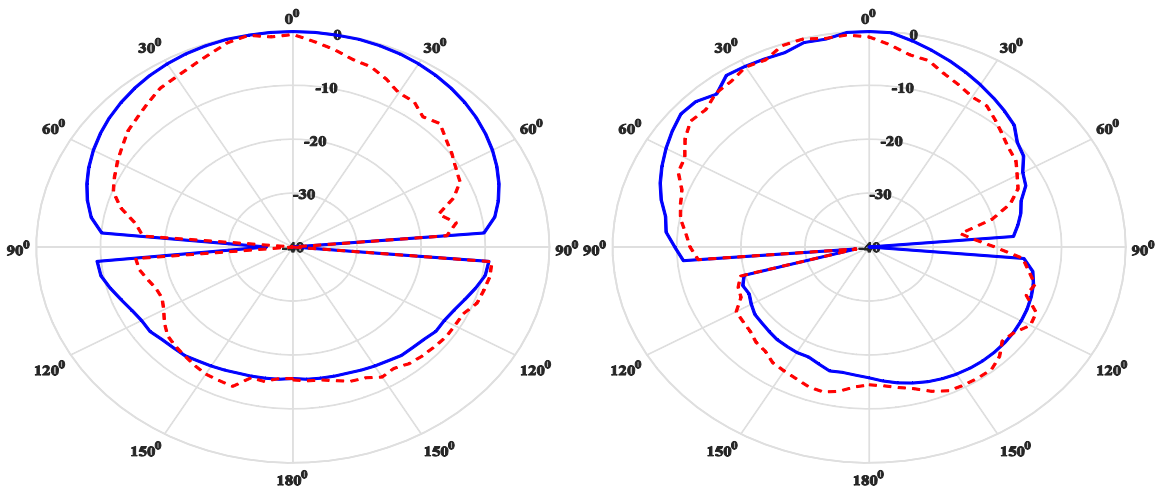

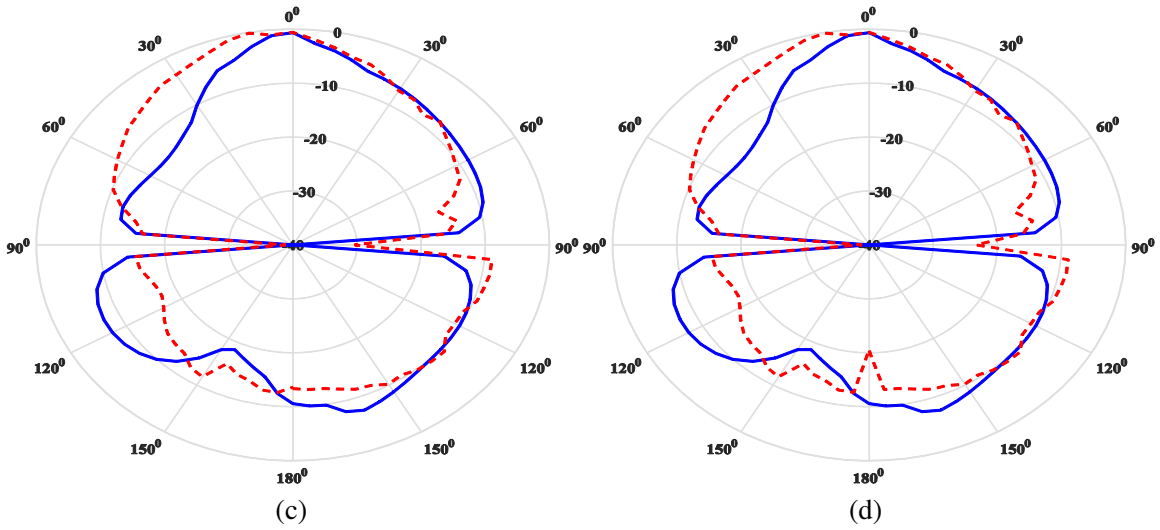

Figure 9. E-plane (X-O-Z plane) radiation characteristics of the proposed antenna. (Solid blue curve: simulated E-Co Poln.; Dashed red curve: measured E-Co Poln). (a) 2.05 GHz, (b) 2.76 GHz, (c) 3.80 GHz, (d) 6.50 GHz.

Table 2. Comparison of the presented antenna with state-of-the-art published work.

Ref. No.	Area	No. of bands	Center Frequency (GHz)	FBR (dB)	Peak gain (dBi)	Additional remarks
[8]	$0.058\lambda^2$	02	1.1, 3.7	8.3@1.1 GHz	4.2, 5.2	Compact and dual-wideband
[22]	$0.286\lambda^2$	02	1.85, 2.53	14, 15	6.14, 6.8	Dual band operation
[23]	$0.630\lambda^2$	02	9.62, 11.13	–	8	Dual wideband operation
[24]	$0.094\lambda^2$	02	0.8665, 0.915	–	2.2	Compact and dual band operation
[25]	$0.459\lambda^2$	02	1.8, 2.6	22, 18.4	6, 7.7	Optimized gain for LTE applications
[26]	$0.168\lambda^2$	02	2.35, 5.195	10.26, 6.7	6.87, 7.7	Dual band operation
[27]	$0.117\lambda^2$	03	1.9, 2.5, 3.5	10.8, 13, 13.1	6.29, 4.63, 6.77	Multiband RADAR application
[28]	$0.120\lambda^2$	03	3.9, 5.62, 8.27	18, 15, 9	4.67, 2.83, 4.19	Multiband applications
[29]	-	04	23.7, 26.3, 27.9, 29.4	–	19.6, 10.5, 16, 11.5	SIW/silicon substrate based antenna, multiband antenna
This Work	$0.192\lambda^2$	04	2.05, 2.75, 3.8, 6.5	14, 13, 12, 19	2, 1.3, 3.1, 3.3	Multiband applications

are 2 dB, 1.3 dB, 3.1 dB, and 3.3 dB, respectively (Figure 8).

The radiation patterns of the fabricated prototype were measured in an anechoic chamber. The measured radiation patterns are plotted in Figures 9 and 10. From these figures it may be noted that measured results are in line with the simulated values. These patterns have good front to back ratios corresponding to four resonant frequencies of 14 dB, 13 dB, 12 dB, and 19 dB, respectively.

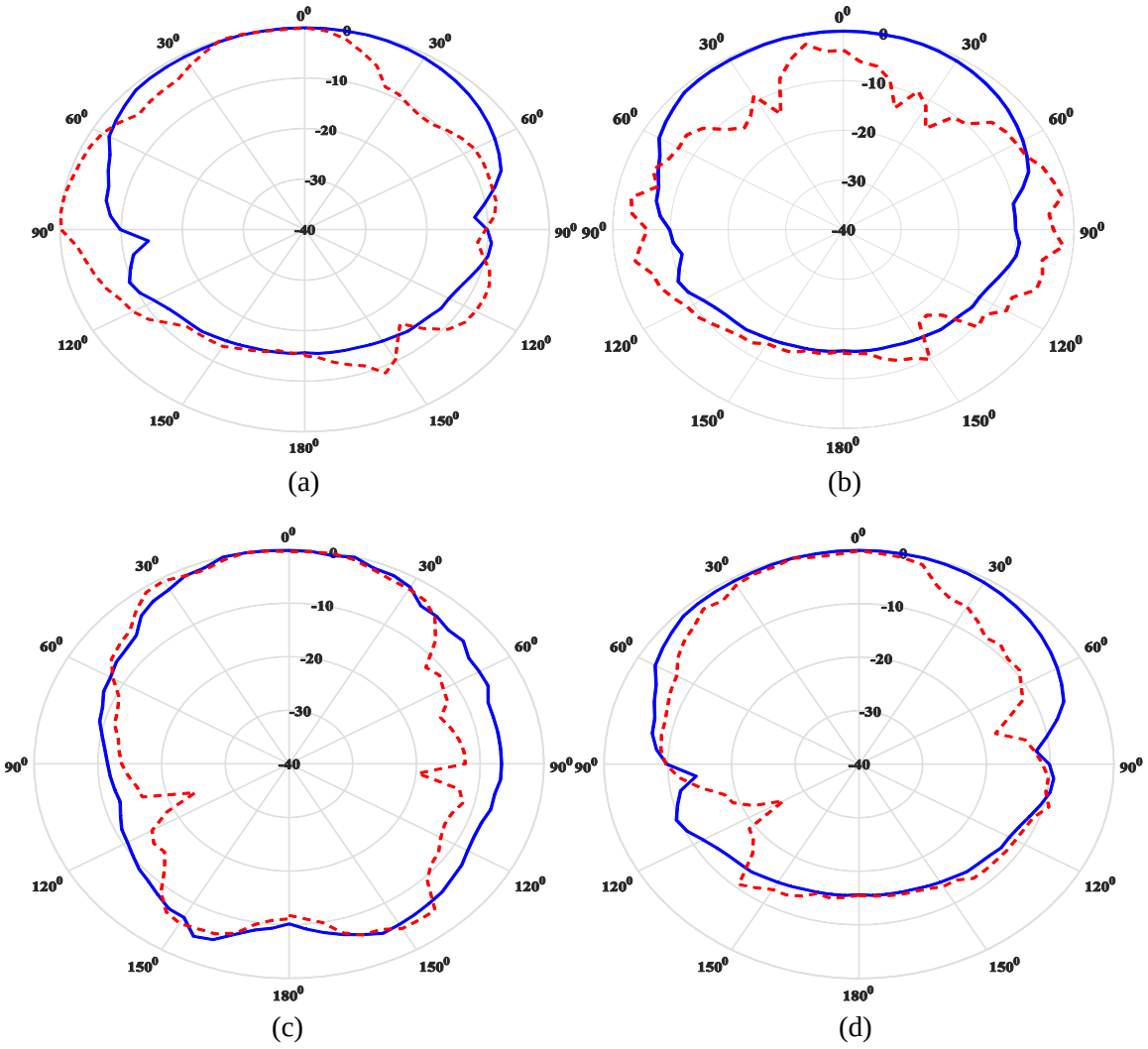

Figure 10. H-plane (Y-O-Z plane) radiation characteristics of the proposed antenna. (Solid blue curve: simulated H-Co Poln.; Dashed red curve: measured H-Co Poln). (a) 2.05 GHz, (b) 2.76 GHz, (c) 3.80 GHz, (d) 6.50 GHz.

To justify, the design proposed here is compared with the state-of-the-art published works. These data are summarized in Table 2. From Table 2 it is worth noting that the proposed antenna presented here is simple to design and offers four operating bands.

5. CONCLUSIONS

A multi-band quasi Yagi antenna which offers four resonant bands is fabricated on a low cost FR-4 substrate, and its input characteristics are tested. Return-loss characteristics, antenna gain, radiation patterns in E-plane and H-plane, and front-to-back (FBR) ratios are measured and validated with their simulation results. The proposed antenna offers four resonant frequencies centered at 2.05 GHz, 2.75 GHz, 3.8 GHz, and 6.5 GHz suitable for various wireless applications including WLAN and 5G services. Front to back ratios are reasonably good at all frequencies. Among the four resonant modes, the last band exhibits wideband characteristics with an impedance bandwidth of 19.27%. The antenna demonstrated here has good front to back ratios of 14 dB, 13 dB, 12 dB, and 19 dB corresponding to four consecutive resonant bands. With these parameters the presented antenna is suitable for WLAN, LTE, RF energy harvesting, and 5G wireless services.

ACKNOWLEDGMENT

The authors thank Prof. K. J. Vinoy, Chairman, ECE Dept., IISc, Bangalore and his students for providing measurement laboratory facilities. Authors also would like to thank Physics Dept. of Central University of Karnataka and IIT Dhanbad for providing Network Analyzer and Anechoic chamber for verification of results.

REFERENCES

1. Gaya, S., R. Hussain, M. S. Sharawi, and H. Attia, "Pattern reconfigurable Yagi-Uda antenna with seven switchable beams for Wi-MAX application," *Microwave Optical Technology Letters*, 1–6, 2019.
2. Hachi, A., H. Lebbar, and M. Himdi, "3D printed large bandwidth new Yagi-Uda antenna," *Progress In Electromagnetic Research Letters*, Vol. 88, 129–135, 2020.
3. Zou, X.-J., G.-M. Wang, Y.-W. Wang, and B.-F. Zong, "Mutual coupling reduction of quasi-Yagi antenna array with hybrid wideband decoupling structure," *International Journal of Electronics and Communications*, Vol. 129, 2021.
4. Chaudhari, A. D. and K. P. Ray, "Compact broadband printed quasi-Yagi antenna with series fed double monopole," *Microwave Optical Technology Letters*, 1–8, 2020.
5. Huang, J. and A. C. Densmore, "Microstrip Yagi array antenna for mobile satellite vehicle application," *IEEE Transactions on Antennas and Propagation*, Vol. 39, No. 7, 1024–1030, Jul. 1991.
6. Yang, L. and J.-J. Zhuang, "Compact quasi-Yagi antenna with enhanced bandwidth and stable high gain," *Electronic Letters*, Vol. 56, No. 5, 219–220, 2020.
7. Kumar, H. and G. Kumar, "Compact planar Yagi-Uda antenna with improved characteristics," *EUCAP*, 2017.
8. Liang, Z. and J. Yuan, "A compact dual-wideband multi-mode printed quasi-Yagi antenna with dual-driven elements," *IET Microwaves Antennas & Propagation*, Vol. 14, No. 7, 1–8, 2020.
9. Ta, S. X., C. D. Bui, and T. K. Nguyen, "Wideband quasi-Yagi antenna with broad-beam dual-polarized radiation for indoor access points," *ACES Journal*, Vol. 34, No. 5, 654–660, 2019.
10. Floc'h, J.-M. and A. El Sayed Ahmad, "Broadband quasi-Yagi antenna for Wi-Fi and Wi-Max applications," *Wireless Engineering and Technology*, Vol. 4, 87–91, 2013.
11. Kumar, H. and G. Kumar, "A broadband planar modified quasi-Yagi using log-periodic antenna," *Progress In Electromagnetic Research Letters*, Vol. 73, 23–30, 2018.
12. Chaudhari, A. D. and K. P. Ray, "Printed broadband quasi-Yagi antenna with monopole elements," *IET Microwaves, Antennas & Propagation*, Vol. 14, No. 6, 468–473, 2020.
13. Ashraf, M. A., K. Jamil, A. Telba, M. A. Alzabidi, and A. R. Sebak, "Design and development of a wideband planar Yagi antenna using tightly coupled directive element," *Micromachines*, Vol. 11, 1–15, 2020.
14. Chaudhari, A. D. and K. P. Ray, "Broadband printed quasi-Yagi antenna with simple feeding structure," *2020 IEEE International Symposium on Antennas and Propagation and North American Radio Science Meeting*, 1921–1922, 2020.
15. Cai, R.-N., M.-C. Yang, S. Lin, X.-Q. Zhang, X.-Y. Zhang, and X.-F. Liu, "Design and analysis of printed Yagi-Uda antenna and two-element array for WLAN applications," *International Journal of Antennas and Propagation*, 1–8, 2012.
16. Mohammed, J. R., "Design of printed Yagi antenna with additional driven element for WLAN applications," *Progress In Electromagnetics Research C*, Vol. 37, 67–81, 2013.
17. Esmail, B. A. F., H. A. Majid, M. F. Ismail, F. Ghawbar, Z. Z. Abidin, and N. Al-Fadhali, "Dual beam Yagi antenna using novel metamaterial structure at 5G band of 28 GHz," *2021 IEEE Symposium on Wireless Technology & Applications (ISWTA)*, 2–5, 2021.
18. Bulla, G., M. T. Le, A. A. A. de Salles, and T. P. Vuong, "Miniaturized printed Yagi antenna for 2.45 GHz RFID readers," *PIERS Proceedings*, 822–824, Marrakesh, Morocco, Mar. 20–23, 2011.

19. Kasabegoudar, V. G. and S. Shirabadagi, "Quasi Yagi for state of the art applications," *International Journal of Engineering Trends and Technology*, Vol. 70, No. 4, 1–14, 2022.
20. Guo, H. and W. Geyi, "Design of Yagi-Uda antenna with multiple driven elements," *Progress In Electromagnetics Research C*, Vol. 92, 101–112, 2019.
21. Zhao, T., Y. Xiong, X. Yu, H. Chen, M. He, L. Ji, X. Zhang, X. Zhao, H. Yue, and F. Hu, "A broadband planar quasi-Yagi antenna with a modified bow-tie driver for multi-band 3G/4G applications," *Progress In Electromagnetics Research C*, Vol. 71, 59–67, 2017.
22. Chen, Z., M. Zeng, A. S. Andrenko, Y. Xu, and H.-Z. Tan, "A dual-band high-gain quasi-Yagi antenna with split-ring resonators for radio frequency energy harvesting," *Microwave Optical Technology Letters*, 1–8, 2019.
23. Qian, Z., L. Yang, and J. Chen, "Design of dual-wide-band quasi-Yagi antenna based on a dielectric resonator," *IEEE Access*, Vol. 8, 16934–16940, 2020.
24. Abdullah, M. H., A. Marzuki, and M. T. Mustaffa, "Design of unlicensed dual band Quasi-Yagi antenna using semi-bowtie for indoor wireless power transfer application," *Journal of Communications*, Vol. 16, No. 12, 2021.
25. Elahi, M., Irfanullah, R. Khan, A. A. Al-Hadi, S. Usman, and P. J. Soh, "A dual-band planar quasi Yagi-Uda antenna with optimized gain for LTE applications," *Progress In Electromagnetics Research C*, Vol. 92, 239–250, 2019.
26. Maurya, N. K. and R. Bhattacharya, "CPW-fed dual-band compact Yagi-type pattern diversity antenna for LTE and Wi-Fi," *Progress In Electromagnetics Research C*, Vol. 107, 183–201, 2021.
27. Cheong, P., K. Wu, W. Choi, and K. Tam, "Yagi-Uda antenna for multiband radar applications," *IEEE Antennas and Wireless Propagation Letters*, Vol. 13, 1065–1068, 2014.
28. Xu, K. D., D. Li, Y. Liu, and Q. H. Liu, "Printed quasi-Yagi antennas using double dipoles and stub-loaded technique for multi-band and broadband applications," *IEEE Access*, Vol. 6, 31695–31702, 2018.
29. Chakraborty, A. and S Srivastava, "High gain substrate integrated waveguide fed Yagi-Uda antenna array on silicon substrate for multiband applications," *Progress In Electromagnetics Research C*, Vol. 116, 265–275, 2021.
30. Cebik, L. B. and W4RNL (SK), "Log periodic arrays," R. D. Straw, N6BV, ed., *The ARRL Antenna Book*, 21st Edition, 10.1–10.28, The American Radio Relay League, Inc., 2007.
31. Carrel, R., "The design of log-periodic dipole antennas," *1958 IRE International Convention Record*, Vol. 9, 61–75, Mar. 21–25, 1966.